The submillimeter rotation tunneling spectrum of $(D_2O)_2$

E. Zwart, J.J. ter Meulen and W. Leo Meerts

Fysisch Laboratorium, University of Nijmegen, Toernooiveld, 6525 ED Nijmegen, The Netherlands

By direct absorption of submillimeter radiation in a planar supersonic jet, we have measured $K_a=1 \rightarrow K_a=2$ transitions of the fully deuterated water dimer $(D_2O)_2$ in the region between 350 and 430 GHz. Several previously unknown constants have been derived. The A-rotational constant is determined as 120327.492(32) MHz. The sum or the difference of the largest tunneling splittings for $K_a=1$ and $K_a=2$ is approximately 21 GHz. The tunneling matrix element h_{2v} has been found to be a factor of 100 smaller than in $(H_2O)_2$.

1. Introduction

The water dimer, $(H_2O)_2$, has been the subject of extensive studies during the past years (see refs. [1,2], and references therein). It has been found that the vibrational ground state splits into six states as a result of tunneling. In fig. 1 this splitting is drawn schematically. Each of the six vibrational tunneling levels has its own rotational structure, which is that of a near-prolate symmetric top. The rotational structure is only indicated by drawing the first two K_a levels. The various J levels for one K_a are rather
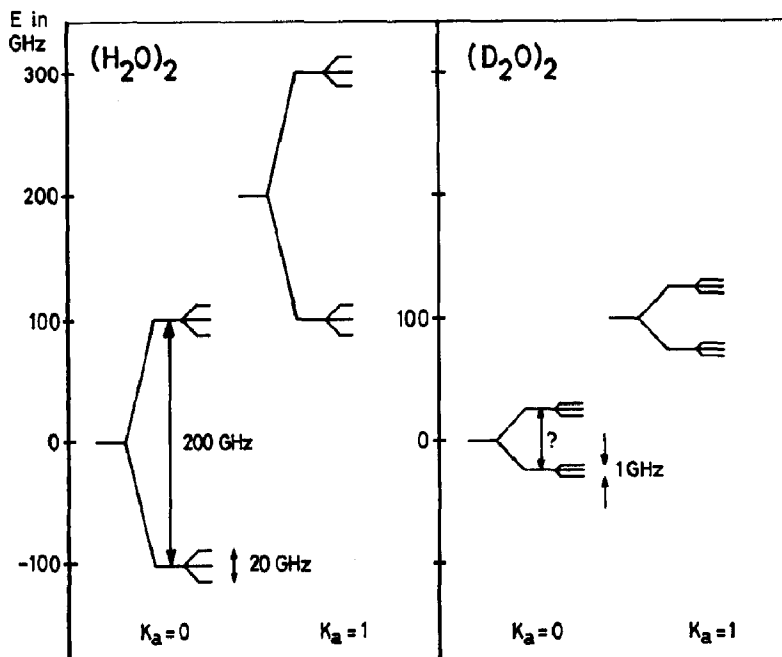

Fig. 1. Energy-level diagram of the lowest levels of $(H_2O)_2$ and $(D_2O)_2$.

close together and are not drawn.

In a first approximation this splitting can be described by two tunneling motions. The tunneling motion with the lowest barrier corresponds to a 180° rotation of the hydrogen-accepting H_2O monomer as a result of which the two hydrogen atoms are interchanged. This splits the vibrational ground state into two states, separated by approximately 200 GHz. These states are split again into three states by the interconversion tunneling motion in which the hydrogen donor/acceptor roles of the two H_2O monomers are interchanged. The result is a state shifted upward, a state shifted downward and a (doubly degenerate) state which is not shifted from the position without interconversion tunneling. The energy difference between the two nondegenerate states is usually called the interconversion tunneling splitting and amounts approximately to 20 GHz.

The fully deuterated species, $(D_2O)_2$, probably has a similar energy-level scheme. However, the tunneling splittings will be smaller. The expected energy level diagram is also drawn in fig. 1. In the theoretical model developed by Coudert and Hougen [3], which was used to fit all available experimental data of $(H_2O)_2$, a high tunneling barrier was assumed. In particular for the internal rotation of the hydrogen-accepting H_2O monomer, there may be some doubt about this assumption. The fully deuterated water dimer, $(D_2O)_2$, will be a good candidate to test the high-barrier assumption.

Until now, only microwave measurements have been reported for $(D_2O)_2$ [4–7]. Dyke et al. [4] have measured $\Delta J = 1$ rotational transitions for $K_a = 2$ and $K_a = 3$, and $\Delta J = 0$ rf transitions for $K_a = 2$. Coudert et al. [5] and Odutola et al. [6] have measured $\Delta J = 1$ rotational and rotational–tunneling transitions for $K_a = 0$. Suenram et al. [7] have extended the previous work. They have measured many transitions for $K_a = 0$ and $K_a = 1$. Transitions in all symmetry states were found. As a result of these microwave measurements, for many rotational constants accurate values are known for the various tunneling levels for $K_a = 0$ and $K_a = 1$; in addition, the interconversion tunneling splittings have been determined. The latter turned out to be approximately 1 GHz, i.e. a factor of 20 smaller than in $(H_2O)_2$. Since no $\Delta K_a = 1$ transitions were measured, the A-rotational constant and the largest tunneling split-

ting are not known precisely from the rotational data.

In this Letter we present measurements of submillimeter transitions from $K_a = 1$ to $K_a = 2$. We have found four of the six possible bands. With these new results, the A-rotational constant is obtained and several tunneling splittings are derived or estimated.

2. Experimental

The spectrometer used in this work has been described in detail in refs. [2,8,9]. The radiation used in this work is produced by generating harmonics of microwave radiation from klystrons. Most lines have been measured with the sixth harmonic of a 60 GHz klystron. The tuning range of the fundamental is 10 GHz and its power 100 mW. The harmonics are generated in an open-structure multiplier with a Schottky barrier diode and radiated in free space by an antenna. The harmonic needed for the experiment is filtered out with a monochromator. The radiation is detected by a 1.5 K Si bolometer in a direct absorption experiment.

The dimers are formed in a continuous expansion of Ar and D_2O, produced with a slit nozzle. The slit is 4 cm long and 15 μm wide. The backing pressure is 500 Torr and the pressure in the vacuum chamber 0.05 Torr. The vacuum chamber is pumped by a 4000 m^3/h roots pump. By passing Ar over D_2O, we produce a gas mixture with a few per cent. D_2O in Ar.

The S/N ratio of the measured lines was at most 10 with an RC time of 3 s.

3. Results

In order to facilitate the understanding of the observed bands, the $K_a = 1$ and $K_a = 2$ levels are drawn with enlarged tunneling splittings in fig. 2. The symmetries in the figure are the symmetries of the rotational–vibrational tunneling wavefunctions in G_{16} [10]. For $K_a > 0$, each state is split due to asymmetry splitting and the following rules hold for the symmetries of the two components of a K-type doublet: For the upper component the symmetry on the left (right) must be taken for J even (odd). For the lower component the symmetry on the left (right) must be taken for J odd (even). $E^{\pm}$ levels between $A_1^{\pm}$, $B_1^{\pm}$
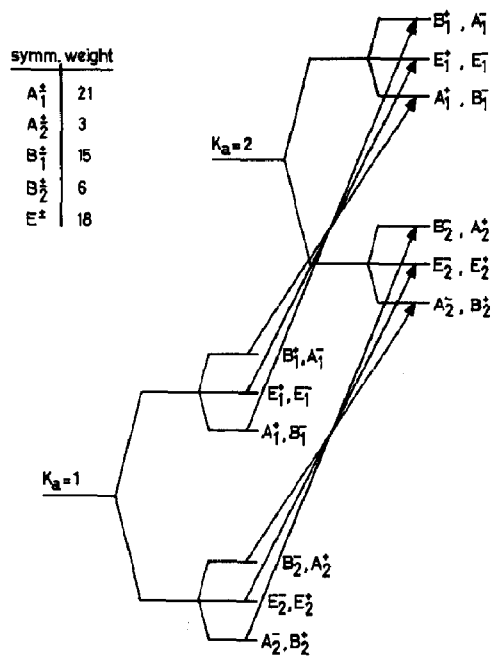
Fig. 2. Energy-level diagram for the $K_a=1$ and $K_a=2$ levels of $(D_2O)_2$. The allowed transitions between vibrational tunneling states and the symmetries of the rotational–vibrational tunneling wavefunctions and their statistical weights are also given. For the symmetries of the two components of a K-type doublet, the following rules hold: For the upper component the symmetry on the left (right) must be taken for J even (odd). For the lower component the symmetry on the left (right) must be taken for J odd (even).

levels are called $E_1^\pm$ and $E^\pm$ levels between $A_2^\pm$, $B_2^\pm$ levels are called $E_2^\pm$. $E_1^\pm$ and $E_2^\pm$ are not symmetries from G_{16}, but are convenient to distinguish the various $E^\pm$ levels [7,11]. Also given in the figure are the statistical weights. Selection rules for electric dipole transitions are $E_1^\pm \leftrightarrow E_1^\mp$, $E_2^\pm \leftrightarrow E_2^\mp$, $A_1^\pm \leftrightarrow A_1^\mp$, $A_2^\pm \leftrightarrow A_2^\mp$, $B_1^\pm \leftrightarrow B_1^\mp$, $B_2^\pm \leftrightarrow B_2^\mp$. Transitions $E_1^\pm \leftrightarrow E_2^\mp$ are not forbidden, but are assumed to be very weak in the high-barrier limit [11]. The various transitions between $K_a=1$ and $K_a=2$ are drawn. Each arrow indicates a set of transitions following the above symmetry selection rules and the additional selection rules $\Delta J=0$, ± 1. It is clear that the spectrum will consist of six bands, similar to vibrational bands, with P, Q and R branches. We will denote the bands by the symmetries of the initial states (e.g. (A_1^+, B_1^-)), and a line from a band by the J tran-

sition and the symmetry of the initial state (e.g. $R(4)A_1^+$). We have found four of the six possible bands. The other bands are probably too weak to observe.

It should be noted that the sign of the largest tunneling splitting cannot unambiguously be determined by theory, and further that this sign can be different for different K_a. This will be discussed in the next section.

Fig. 3 is a part of the Q branch of the (A_1^+, B_1^-) band. This represents only one half of the Q branch. (In this part the lines are rather close together.) Due to asymmetry doubling, every line from a band appears twice. Because of the low intensity of the lines, the bands were not found in initial, fast scans. In that case only Ar–D_2O bands were observed [12]. Next, in slow scans, a few lines of $(D_2O)_2$ were detected. To distinguish them from lines of complexes with Ar, we replaced Ar by Kr. With the help of the known microwave transitions and their spectroscopic constants, the other lines could be predicted and were then found. The asymmetry constants for $K_a=1$ from ref. [7] were especially helpful in assigning the observed spectra. (The asymmetry splittings in $K_a=2$ are small.)

We were only able to detect Q- and R-branch transitions. No P-branch lines were detected, though their positions are very accurately known from combination differences with microwave results. For $(H_2O)_2$ it was found [9,13] that the P lines are a few times weaker than Q or R lines. From fig. 3 it is clear,
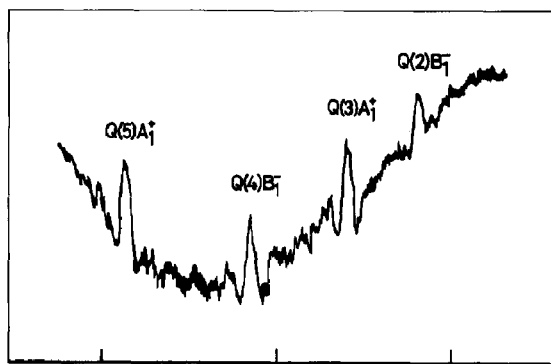

Fig. 3. Part of the Q branch of the (A_1^+, B_1^-) band. The RC time is 3 s. The distance between the frequency markers is 10 MHz.

that we cannot afford to loose more than a factor of 3 in intensity. We therefore assume that the sensitivity is too low to detect P-branch lines.

For the two bands of the $E^{\pm}$ levels, microwave measurements have been made in both initial and final states, so for these bands combination differences can be used to check our assignments. The combination differences agreed to within 0.1 MHz, which is approximately the accuracy of our frequency measurements. For the other two bands only microwave measurements in the initial states are available, so only combination differences can be calculated between two submillimeter transitions with a common upper state. Unfortunately, this was not possible for the present results because of the lack of P lines.

Additionally the relative intensities of the observed transitions confirm the assignments. Lines in the bands of $E^{\pm}$ symmetry show no intensity alternation, whereas the other two bands have an intensity alternation. The latter was to be expected from the ratio of statistical weights of $A_1^{\pm}$ and $B_1^{\pm}$ symmetry 21/15. Due to the low intensity of the lines, the exact intensity ratio is difficult to measure. However, a comparison of the strengths of two lines from a K-type doublet clearly shows intensity alternations. Furthermore, bands which could not be detected are, due to their statistical weights, appreciably weaker than the observed ones. (See fig. 2.)

The four bands were fitted separately to a near-prolate symmetric-top formula. The same procedure was used by Suenram et al. [7]. The transitions were assumed to be c-type. The constants, given in table 5, have their usual meanings. The parameter d is the distortion in the asymmetry constant for $K_a = 1$. The constant c describes the asymmetry splitting in $K_a = 2$ and is the same as used by Dyke et al. [4], i.e. the asymmetry splitting in $K_a = 2$ is given by $c(J-1)$ $\times J(J+1)(J+2)$. In all cases we obtained acceptable fits as can be seen from tables 1–4. The resulting parameters are listed in table 5.

4. Discussion

The standard deviations of the fits are somewhat smaller than the estimated uncertainty of the measured frequencies. The constants from the fit agree

Table 1
Observed and calculated frequencies for the (E_2^-, E_2^+) band in MHz

Transition	Observed	Obs. − calc.
$Q(2)E_2^-$	350543.41	−0.01
$Q(2)E_2^+$	350722.40	−0.02
$Q(3)E_2^+$	350439.37	0.00
$Q(3)E_2^-$	350797.43	0.00
$Q(4)E_2^-$	350300.63	0.04
$Q(4)E_2^+$	350897.51	0.02
$Q(5)E_2^+$	350127.00	−0.02
$Q(5)E_2^-$	351022.61	−0.03
$Q(6)E_2^-$	349918.63	0.00
$Q(6)E_2^+$	351172.94	0.01
$R(1)E_2^+$	372324.02	0.02
$R(1)E_2^-$	372383.62	0.00
$R(2)E_2^-$	383108.23	0.00
$R(2)E_2^+$	383286.97	−0.01
$R(3)E_2^+$	393855.36	−0.03
$R(3)E_2^-$	394212.61	−0.01
$R(4)E_2^-$	404564.74	0.00
$R(4)E_2^+$	405159.59	0.02
$R(5)E_2^+$	415235.58	0.00
$R(5)E_2^-$	416126.84	−0.01

Table 2
Observed and calculated frequencies for the (E_1^+, E_1^-) band in MHz

Transition	Observed	Obs. − calc.
$Q(2)E_1^+$	371248.93	0.02
$Q(2)E_1^-$	371348.24	−0.02
$Q(3)E_1^-$	371154.70	0.00
$Q(3)E_1^+$	371353.46	0.03
$Q(4)E_1^+$	371029.15	−0.04
$Q(4)E_1^-$	371360.50	0.02
$Q(5)E_1^-$	370872.50	0.02
$Q(5)E_1^+$	371369.52	−0.02
$R(1)E_1^-$	393012.64	0.01
$R(1)E_1^+$	393045.73	−0.01
$R(2)E_1^+$	403798.16	−0.03
$R(2)E_1^-$	403897.49	0.01
$R(3)E_1^-$	414549.95	0.00
$R(3)E_1^+$	414748.48	0.01
$R(4)E_1^+$	425267.19	0.01
$R(4)E_1^-$	425597.94	−0.01

very well with those obtained from refs. [4,7]. This proves that the assignment of the two bands which could not be checked with combination differences must be correct. From the results of the fit several

Table 3
Observed and calculated frequencies for the (B_1^+, A_1^-) band in MHz

Transition	Observed	Obs. − calc.
$Q(2)B_1^+$	370282.21	0.00
$Q(2)A_1^-$	370381.32	0.03
$Q(3)A_1^-$	370189.67	0.02
$Q(3)B_1^+$	370387.86	−0.02
$Q(4)B_1^+$	370066.38	0.00
$Q(4)A_1^-$	370396.80	−0.03
$Q(5)A_1^-$	369912.50	−0.01
$Q(5)B_1^+$	370408.33	0.02
$R(1)A_1^-$	392045.05	−0.02
$R(1)B_1^+$	392078.06	−0.03
$R(2)B_1^+$	402831.91	0.06
$R(2)A_1^-$	402930.86	−0.02
$R(3)A_1^-$	413585.42	−0.01
$R(3)B_1^+$	413783.45	0.02
$R(4)B_1^+$	424305.09	−0.01
$R(4)A_1^-$	424635.00	0.00

Table 4
Observed and calculated frequencies for the (A_1^+, B_1^-) band in MHz

Transition	Observed	Obs. − calc.
$Q(2)A_1^+$	372164.77	−0.01
$Q(2)B_1^-$	372264.07	−0.04
$Q(3)B_1^-$	372069.49	0.04
$Q(3)A_1^+$	372268.17	0.02
$Q(4)A_1^+$	371942.44	−0.01
$Q(4)B_1^-$	372273.67	−0.02
$Q(5)B_1^-$	371783.88	0.00
$Q(5)A_1^+$	372280.87	0.01
$R(1)B_1^-$	393929.15	0.00
$R(1)A_1^+$	393962.28	0.03
$R(2)A_1^+$	404713.88	−0.02
$R(2)B_1^-$	404813.17	0.00
$R(3)B_1^-$	415464.45	−0.01
$R(3)A_1^+$	415662.96	0.00
$R(4)A_1^+$	426180.13	0.01
$R(4)B_1^-$	426510.84	0.00

Table 5
Molecular constants of $(D_2O)_2$ and their errors obtained from the least squares fit of the various bands. The errors in the constants are the errors which result from the estimated uncertainty in the observed frequencies (0.1 MHz). The standard deviations are approximately a factor of 4 smaller. ν_0 (band origin), $\bar{B}''$, $\bar{B}'$, $B'' - C''$ and σ (stand. dev.) in MHz. D'', D', d'' and c' in kHz

	(E_2^-, E_2^+)	(E_1^+, E_1^-)	(B_1^+, A_1^-)	(A_1^+, B_1^-)
ν_0	350647.442(84)	371343.19(11)	370374.85(11)	372260.18(11)
$\bar{B}''$	5430.505(14)	5432.934(18)	5432.740(18)	5433.100(8)
D''	35.45(25)	35.55(47)	35.51(47)	35.79(47)
$B'' - C''$	59.661(16)	33.1133(64)	33.0282(64)	33.1079(64)
d''	0.42(12)			
$\bar{B}'$	5428.085(15)	5425.493(22)	5425.549(22)	5425.471(22)
D'	35.46(26)	34.40(53)	34.10(53)	34.59(53)
c'	1.722(62)	0.43(11)	0.45(11)	0.43(11)
σ	0.017	0.019	0.022	0.019

constants which were previously unknown can be derived. This will be discussed below and the results are summarized in table 6.

The interconversion tunneling splitting between (A_1^+, B_1^-) and (B_1^+, A_1^-) levels for $K_a = 2$ can easily be calculated and the result is 808.72(16) MHz. Comparing this splitting with those for $K_a = 0$ (1172 MHz) and $K_a = 1$ (1077 MHz), we find that it strongly decreases with increasing K_a. A similar re-

Table 6
Constants and their errors obtained from the observed bands. $\Delta\nu_{int}$ is the interconversion tunneling splitting between (A_1^+, B_1^-) and (B_1^+, A_1^-) levels for $K_a = 2$. All quantities are in MHz

Constant	Value
$\Delta\nu_{int}$	808.72(16)
$h_{2\nu}$	−6.420(34)
A	120327.492(32)

sult was found for $(H_2O)_2$.

There exists another tunneling motion in the water dimer in which the hydrogens of the hydrogen-donating water monomer are interchanged. This tunneling motion causes shifts of the energy levels. Coudert and Hougen [14] proposed that for $(H_2O)_2$ and $(D_2O)_2$, levels of E symmetry are moved upward for K_a even and downward for K_a odd, respectively. For levels of A and B symmetry, the levels shift downward and upward for K_a even and odd, respectively. If we neglect the dependence on the rotational tunneling state this shift is given by $|h_{2v}|$. Here h_{2v} is a matrix element from ref. [14], whose value is proposed to be negative. It will be clear that as a result of this tunneling motion, the $K_a = 1 \rightarrow 2$ bands will be shifted upward (E levels) or downward (A, B levels) by $2 |h_{2v}|$. The band origins yield $|h_{2v}|$. From the results of table 5, we calculate $h_{2v} = -6.420(34)$ MHz. This value is approximately a factor of 100 smaller than in $(H_2O)_2$ [15].

If one neglects the dependence of the tunneling shift, described by h_{2v}, on the rotational–tunneling state, the mean of the band origins of the two bands of E symmetry, $\bar{\nu}$, obeys

$$\bar{\nu} = 3A + |2h_{2v}|,$$

where A is the rotational constant along the a axis.

Substituting $\bar{\nu}$ and h_{2v} in this equation, we find $A = 120327.492(32)$ MHz.

Probably the most interesting quantity which cannot be determined from microwave spectroscopy concerns the largest tunneling motion for $(D_2O)_2$. From the submillimeter results, we can obtain information about this quantity. However, there is some ambiguity which depends on the ordering of the levels. There are three possibilities, depicted in fig. 4: In fig. 4a the ordering for $K_a = 1$ is the same as in $(H_2O)_2$. This assumption is supported by the observation that transitions in the (E_2^+, E_2^-) band are approximately 1.5 times stronger than those in the (E_1^+, E_1^-) band. Fig. 4a implies that the tunneling splitting in $K_a = 2$ is 21 GHz larger than the tunneling splitting in $K_a = 1$. If the levels are ordered as in fig. 4b the splitting in $K_a = 2$ is 21 GHz smaller than the splitting in $K_a = 1$, i.e. a decrease of the tunneling splitting is found similar to that for the interconversion tunneling splitting. The ordering in fig. 4c implies that the sum of the splittings in $K_a = 1$ and $K_a = 2$ is 21 GHz. In that case, the tunneling splitting would be a factor of 20 smaller than for $(H_2O)_2$, which is the same factor as for the interconversion tunneling splitting. Though we have a weak preference for the assumption of fig. 4a, we cannot unambiguously prove either of the assumptions.
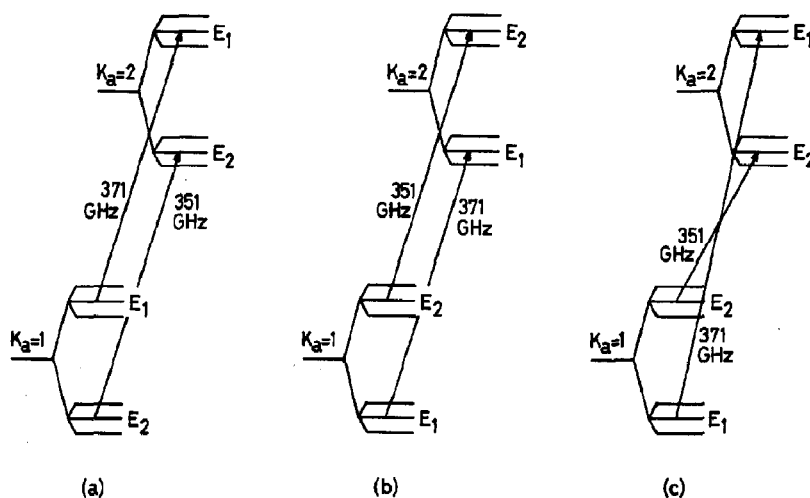

Fig. 4. The various possible assignments of the observed bands. E_1 and E_2 denote the levels for which the possible rotational–vibrational tunneling symmetries are $E_1^\pm$ and $E_2^\pm$, respectively.

References

[1] G.T. Fraser, Intern. Rev. Phys. Chem., to be published.
[2] E. Zwart, J.J. ter Meulen and W.L. Meerts, Chem. Phys. Letters 166 (1990) 500.
[3] L.H. Coudert and J.T. Hougen, J. Mol. Spectry. 139 (1990) 259.
[4] T.R. Dyke, K.M. Mack and J.S. Muenter, J. Chem. Phys. 66 (1977) 498.
[5] L.H. Coudert, F.J. Lovas, R.D. Suenram and J.T. Hougen, J. Chem. Phys. 87 (1987) 6290.
[6] J.A. Odutola, T.A. Hu, D. Prinslow, S.E. O'Dell and T.R. Dyke, J. Chem. Phys. 88 (1988) 5352.
[7] R.D. Suenram, G.T. Fraser and F.J. Lovas, J. Mol. Spectry. 138 (1989) 440.
[8] P. Verhoeve, E. Zwart, M. Drabbels, M. Versluis, J.J. ter Meulen, A. Dymanus and D. McLay, Rev. Sci. Instr., to be published.
[9] E. Zwart, J.J. ter Meulen, W.L. Meerts and L.H. Coudert, in preparation.
[10] T.R. Dyke, J. Chem. Phys. 66 (1977) 492.
[11] G.T. Fraser, R.D. Suenram and L.H. Coudert, J. Chem. Phys. 90 (1989) 6077.
[12] E. Zwart, J.J. ter Meulen and W.L. Meerts, in preparation.
[13] K.L. Busarow, R.C. Cohen, G.A. Blake, K.B. Laughlin, Y.T. Lee and R.J. Saykally, J. Chem. Phys. 90 (1989) 3937.
[14] L.H. Coudert and J.T. Hougen, J. Mol. Spectry. 130 (1988) 86.
[15] G.T. Fraser, R.D. Suenram, L.H. Coudert and R.S. Frye, J. Mol. Spectry. 137 (1989) 244.